



Engagement of the S1, S1' and S2' subsites drives efficient catalysis of peptide bond hydrolysis by the M1-family aminopeptidase from *Plasmodium falciparum*

Seema Dalal¹, Daniel R.T. Ragheb¹, Michael Klemba*

Department of Biochemistry, Virginia Tech, Blacksburg, VA 24061, USA

ARTICLE INFO

Article history:

Received 8 December 2011

Received in revised form 2 February 2012

Accepted 6 February 2012

Available online 13 February 2012

Keywords:

Malaria
Peptidase
Vacuole
Hemoglobin
Enzyme kinetics

ABSTRACT

The M1-family aminopeptidase PfA-M1 catalyzes the last step in the catabolism of human hemoglobin to amino acids in the *Plasmodium falciparum* food vacuole. In this study, the structural features of the substrate that promote efficient PfA-M1-catalyzed peptide bond hydrolysis were analyzed. X-Ala and Ala-X dipeptide substrates were employed to characterize the specificities of the enzyme's S1 and S1' subsites. Both subsites exhibited a preference for basic and hydrophobic sidechains over polar and acidic sidechains. The relative specificity of the S1 subsite was similar over the pH range 5.5–7.5. Substrate P1 and P1' residues affected both K_m and k_{cat} , revealing that sidechain–subsite interactions not only drive the formation of the Michaelis complex but also influence the rates of ensuing chemical steps. Only a small fraction of the available binding energy was exploited in interactions between substrate sidechains and the S1 and S1' subsites, which indicates a modest level of complementarity. There was no correlation between S1 and S1' specificities and amino acid abundance in hemoglobin. Interactions between PfA-M1 and the backbone atoms of the P1' and P2' residues as well as the P2' sidechain further contributed to the catalytic efficiency of substrate hydrolysis. By demonstrating the engagement of multiple, broad-specificity subsites in PfA-M1, these studies provide insight into how this enzyme is able to efficiently generate amino acids from highly sequence-diverse di- and oligopeptides in the food vacuole.

© 2012 Elsevier B.V. All rights reserved.

1. Introduction

Aminopeptidases catalyze the hydrolysis of the amide bond between the first two residues of a (poly)peptide. In eukaryotes, they have important housekeeping roles in degrading peptides generated by endopeptidases in the cytosol or in degradative organelles such as the yeast vacuole. Aminopeptidases can also perform highly specialized functions, for example by producing or degrading bioactive peptides in higher eukaryotes. Metallo-aminopeptidases of the M1 family are ubiquitous across all kingdoms of life. Of the twelve human M1-family aminopeptidases, several have been linked to pathological processes such as hypertension, inflammation and cancer and have been the targets of inhibitor development efforts [1–3].

Malaria is caused by protozoan parasites of the genus *Plasmodium* as they replicate within the host's erythrocytes. *P. falciparum*,

the most virulent human malaria parasite, is responsible for approximately one million deaths annually [4]. While in the erythrocyte, *P. falciparum* endocytoses two-thirds of the host cell hemoglobin [5] and degrades it to amino acids in an acidic organelle called the food vacuole. Numerous endo- and exopeptidases contribute to hemoglobin catabolism in the vacuole, including two aminopeptidases [6–9]. One of these is a homolog of aminopeptidase P that is highly specific for peptide substrates with a proline in the P1' position² [11]. The other is an M1-family aminopeptidase termed PfA-M1 (for *P. falciparum* Aminopeptidase-M1 family [12]; PlasmoDB ID MAL13P1.56), which is the subject of this study. PfA-M1 is located in the food vacuole and it is an efficient catalyst of peptide hydrolysis at the moderately acidic pH of the vacuole lumen [6,13,14]. We have proposed that PfA-M1 is the primary catalyst of the hydrolytic release of amino acids from globin-derived peptides. Because it is also found in the parasite's nucleus [6,13,14], PfA-M1 may have another function unrelated to hemoglobin catabolism.

Recent chemical genetic studies have provided direct evidence for a role for PfA-M1 in vacuolar hemoglobin catabolism. By

Abbreviations: AccQ-Tag, 6-aminoquinolyl-N-hydroxysuccinimidyl carbamate; IMAC, immobilized metal affinity chromatography; LTA4H, leukotriene A₄ hydroxylase; PfA-M1, *P. falciparum* aminopeptidase-M1 family.

* Corresponding author at: 306 Engel Hall, Department of Biochemistry, Virginia Tech, Blacksburg, VA 24061, USA. Tel.: +1 540 231 5729; fax: +1 540 231 9070.

E-mail address: klemba@vt.edu (M. Klemba).

¹ These authors contributed equally to this work.

² The nomenclature of Schechter and Berger [10] is used here. P1, P1' and P2' refer to substrate residues while S1, S1' and S2' refer to the corresponding enzyme subsites. For aminopeptidases, the scissile peptide bond is between the P1 and P1' residues.

screening libraries of activity-based probes based on the structure of the potent but unspecific aminopeptidase inhibitor bestatin, a probe was identified (*O*-benzyltyrosyl-alanyl probe, referred to as BTA) that was highly specific for PfA-M1 over other *P. falciparum* aminopeptidases [15]. Treatment of cultured *P. falciparum* with BTA caused swelling of the food vacuole and the accumulation of globin peptides in the parasite [15]. BTA was a potent inhibitor of parasite replication (EC_{50} of 1 μ M) [15], which points to an essential role for PfA-M1 in blood-stage parasite proliferation and explains why a previous attempt to disrupt the PfA-M1 gene was unsuccessful [6]. These data, together with results from other inhibitor development efforts [16,17], validate PfA-M1 as a target for the further investigation of inhibitors with anti-malarial properties.

An analysis of the substrate specificity of PfA-M1 would be valuable to better understand its *in vivo* functions and to aid in the design of potent active-site directed inhibitors. The objective of this study was to identify the structural features of the peptide substrate that promote efficient hydrolysis by PfA-M1. The importance of interactions with the S1, S1' and S2' subsites of PfA-M1 was evaluated by systematically varying the P1, P1' and P2' substrate residues, respectively. In addition, the effects on catalysis of altering substrate backbone length were examined. Steady state kinetic parameters were determined for all substrates so that the contributions of the Michaelis constant (K_m) and turnover number (k_{cat}) to the catalytic efficiency could be evaluated. The results provide a clear picture of the suite of enzyme–substrate interactions that drive efficient catalysis by an essential malarial aminopeptidase.

2. Materials and methods

2.1. Reagents

Peptides were obtained from Bachem Americas, Sigma–Aldrich and Peptides International. Stock solutions were made in water and the pH was adjusted to that of the assay (pH 7.5 or 5.5) with sodium hydroxide as necessary. 6-Aminoquinolyl-*N*-hydroxysuccinimidyl carbamate (AccQ-Tag) was obtained from Waters.

2.2. PfA-M1 expression and purification

Recombinant PfA-M1 (residues 192–1085) was expressed in *E. coli* and purified from soluble bacterial lysate as previously described [14] with the following modifications to eliminate carryover of metal ions from the immobilized metal affinity chromatography (IMAC) steps and to enable measurement of Zn(II) stoichiometry of the purified protein. A Co(II)-containing TALON™ column (Clontech) was used for IMAC. After tobacco etch virus protease removal of the hexahistidine tag and reverse IMAC [14], 100 μ M ethylenediaminetetraacetic acid was added to the protein for 4 h at 4 °C to chelate small amounts of Co(II) that presumably originated from the IMAC purifications. The protein was dialyzed overnight at 4 °C against 50 mM Tris–HCl pH 7.5, 200 mM NaCl and 100 μ M ZnCl₂ to remove the ethylenediaminetetraacetic acid and load the protein with Zn(II). Free Zn(II) was separated from PfA-M1 by injecting the dialyzed protein onto a Superdex 200 10/30 gel filtration column equilibrated in 50 mM Tris–HCl pH 7.5, 200 mM NaCl. Fractions containing purified PfA-M1 were pooled, snap frozen in aliquots in liquid nitrogen and stored at –80 °C. PfA-M1 concentration was determined by absorbance at 280 nm using a calculated extinction coefficient of $1.15 \times 10^5 \text{ M}^{-1} \text{ cm}^{-1}$.

2.3. Metal analysis

The metal content of purified recombinant PfA-M1 was analyzed using a Dionex ICS-3000 ion chromatography system, which permits the separation and quantitation of transition metal ions. The

ions were resolved as complexes with pyridine-2,6-dicarboxylic acid on an IonPac CS5A ion exchange column (4 mm \times 250 mm; Dionex) and were detected by absorbance at 530 nm following post-column derivitization with 4-(2-pyridylazo)resorcinol [18]. To release enzyme-bound metals, samples containing 5–10 μ M purified recombinant PfA-M1 in 50 mM Tris–HCl pH 7.5, 200 mM NaCl were mixed with an equal volume of 1 M nitric acid immediately prior to analysis. Standard solutions of Co(II), Ni(II), Zn(II), Fe(III), Cu(II) and Cd(II) were used to identify metal complexes. Amounts of Zn(II) in the PfA-M1 samples were quantified in triplicate by reference to a Zn(II) atomic absorption standard solution (Fluka).

2.4. Determination of kinetic parameters

Rates of peptide hydrolysis were determined in 100 mM sodium HEPES pH 7.5/110 mM NaCl or sodium MES pH 5.5/110 mM NaCl at 30 °C for 15 min. One of the amino acid products (Ala for Ala-X and X-Ala peptides except Pro–Ala, for which Pro was used; Leu for the substrates in Table 3) was quantified as the AccQ-Tag derivative by reverse phase ultra-high pressure liquid chromatography as previously described [14]. For each substrate, an initial scan of concentrations was carried out to estimate the K_m and k_{cat} values. These values were then determined in a minimum of three independent assays using 8 substrate concentrations that ranged from $\sim 0.2 K_m$ to $\sim 5 K_m$. Enzyme amounts were adjusted such that substrate consumption was less than 20%. When very low substrate concentrations were required, up to 30% substrate consumption was tolerated in order to maintain adequate sensitivity. Data points were fit by non-linear regression to the Michaelis–Menten equation $v = V_s/(K_m + s)$ using Kaleidagraph 4.1 (Synergy Software) where V is the limiting velocity and s is the substrate concentration. k_{cat} was calculated from the relationship $V = k_{cat} \cdot e$ where e is the enzyme concentration. The quality of data sets was assessed using the R^2 value and those having R^2 -values less than 0.98 were discarded. Means and standard deviations for K_m , k_{cat} and k_{cat}/K_m were calculated with error propagated for the latter quantity. Statistical significance of differences of means from pairs of substrates was assessed using a two-tailed unpaired Welch's *t*-test. When the K_m values were over 100 mM, k_{cat}/K_m values were estimated by measuring initial rates under conditions where $[S] \ll K_m$ ($[S] = 2, 4$ and 8 mM) and calculating k_{cat}/K_m from the relationship $v = k_{cat}/K_m \cdot e$. Incremental binding free energies were calculated using the formula $\Delta \Delta G_b = -RT \ln((k_{cat}/K_m)_{SUB1}/(k_{cat}/K_m)_{SUB2})$ [19], where SUB1 and SUB2 are substrates 1 and 2 in Table 1, respectively.

3. Results

3.1. Metal content of recombinant PfA-M1

PfA-M1 contains a single Zn(II) ion in the active site [20]. Prior to embarking on a kinetic characterization, we determined the metal content of recombinant PfA-M1 to assess occupancy of the metal site. Analysis of a preparation of recombinant PfA-M1 that was purified as described previously [14] identified Zn(II) as the major metal species but also revealed sub-stoichiometric amounts of Ni(II), which presumably reflects contamination introduced during the Ni(II)-affinity chromatography steps (data not shown). When the purification was modified as described in Section 2.2, PfA-M1 was found to contain 1.2 ± 0.1 equivalents of Zn(II). None of the other transition metals that are detectable with this method (Ni(II), Co(II), Cu(II), Cd(II) and Fe(III)) were present above background levels. To ensure that the PfA-M1–Zn(II) complex was separated from free Zn(II) during the last step of the purification, the gel filtration step was performed with a protein blank and fractions in which

Table 1
Incremental binding free energies ($\Delta\Delta G_b$) of PfA-M1 S1 and S1' subsites with various sidechain groups.

Subsite	Substrate 1	Substrate 2	Group ^c	$\Delta\Delta G_b^a$	Intrinsic $\Delta\Delta G_b^{a,b}$
S1	Leu-Ala	Ala-Ala	—CH ₂ (CH ₃) ₂	−3.4	−40
	Tyr-Ala	Phe-Ala	—OH	1.7	−29
S1'	Ala-Ala	Ala-Gly	—CH ₃	−2.8	−14
	Ala-Ile	Ala-Val	—CH ₃	−2.9	−14
	Ala-Val	Ala-Gly	—CH ₂ (CH ₃) ₂	−4.6	−40
	Ala-Leu	Ala-Ala	—CH ₂ (CH ₃) ₂	−4.1	−40
	Ala-Tyr	Ala-Phe	—OH	−3.4	−29

^a $\Delta\Delta G_b$ values (in kJ/mol) are for the transfer of the indicated groups from water to enzyme.

^b Determined with aminoacyl-tRNA synthetases [19].

^c The group in substrate 1 replaces a hydrogen atom in substrate 2.

PfA-M1 would elute were collected and pooled. These fractions contained a low level of Zn(II) corresponding to ~0.1 molar equivalents of PfA-M1. Thus, the observed stoichiometry is not an artifact of inadequate separation of recombinant PfA-M1 from free Zn(II). These results are consistent with full occupancy of the active site of recombinant PfA-M1 with a single Zn(II) ion. We therefore assume for the purpose of calculating k_{cat} that the enzyme preparation is 100% active. It is, however, formally possible that PfA-M1 is fully loaded with Zn(II) yet less than 100% active. This would result in a

systematic underestimate of k_{cat} that would affect all substrate k_{cat} values to the same extent.

3.2. Characterization of the S1 and S1' subsites

The specificities of the S1 and S1' subsites of PfA-M1 were probed by determining the steady-state kinetic parameters for the hydrolysis of X-Ala and Ala-X substrate sets, respectively, where X represents a diverse range of natural amino acids. Substrates

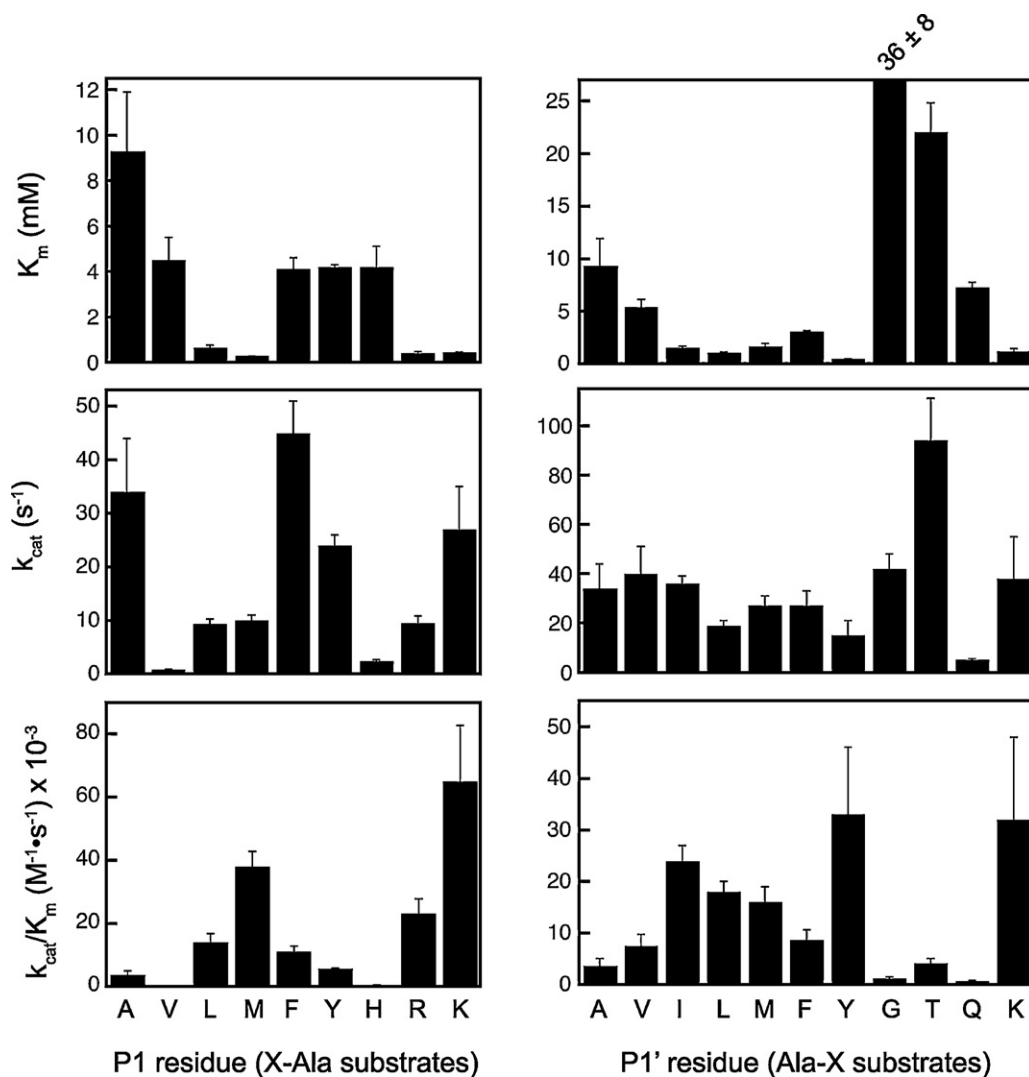


Fig. 1. Steady-state kinetic parameters for PfA-M1-catalyzed hydrolysis of X-Ala (left panels) and Ala-X (right panels) substrate sets. Mean values are shown with standard deviations represented with error bars. Parameters for Ala-Ala are shown in both sets.

Table 2
Kinetic parameters for substrates with backbone and P2' modifications.

Substrate	K_m (mM)	k_{cat} (s^{-1})	k_{cat}/K_m ($M^{-1} s^{-1}$)
Leu-NH ₂	4.9 ± 0.6	12 ± 1	$(2.4 ± 0.4) × 10^3$
Leu-Gly	0.95 ± 0.22	6.5 ± 1.3	$(6.8 ± 2.1) × 10^3$
Leu-Gly-NH ₂	0.42 ± 0.05	21 ± 3	$(4.9 ± 1.0) × 10^4$
Leu-Gly-Gly	0.70 ± 0.16	21 ± 5	$(3.0 ± 1.0) × 10^4$
Leu-Gly-Pro	0.20 ± 0.04	12 ± 2	$(6.0 ± 1.7) × 10^4$
Leu-Gly-Leu	0.015 ± 0.002	4.8 ± 0.3	$(3.3 ± 0.5) × 10^5$

were chosen such that both sets included Gly, Ala, Pro, an extensive group of aliphatic and aromatic hydrophobic residues, and representative basic, acidic and polar residues. All kinetic parameters were determined at 30 °C and, except where indicated below, at pH 7.5. For both substrate sets, rates of hydrolysis were determined from the amount of alanine produced (or proline for Pro-Ala, which was not resolved from the alanine peak). Steady-state kinetic parameters were obtained by non-linear regression fits to the Michaelis–Menten equation. For Gly-Ala, Pro-Ala and Ala-Glu, the K_m values were greater than 100 mM. It was therefore not possible to obtain data sets for fitting to the Michaelis–Menten equation. However, we were able to estimate k_{cat}/K_m from rates obtained under the condition $[S] \ll K_m$ (see Section 2.4). Mean values of steady-state kinetic parameters with standard deviations are provided in Supplemental Table S1 and most of these are represented graphically in Fig. 1.

The identity of the substrate P1 residue had a large effect on the K_m and k_{cat} values for X-Ala dipeptide hydrolysis by PfA-M1 (Fig. 1). The K_m value for Ala-Ala was relatively high at 9.3 mM. All other substrates in Fig. 1 exhibited significantly lower K_m values ($p \leq 0.03$), which indicate that a broad range of non-polar and polar P1 sidechains can establish interactions with residues in the S1 subsite. K_m varied over a 23-fold range, with substrates having aliphatic hydrophobic and basic P1 residues (Leu, Met, Arg and Lys) yielding the lowest values. For non-polar residues, there was a moderate inverse correlation between the K_m value and sidechain hydrophobicity ($R^2 = 0.55$) as assessed by solvation free energies calculated from the octanol–water partitioning of Ac-X-amides at pH 7.1 (Fig. 2 [21]). Variation in k_{cat} (56-fold) was of a similar magnitude to that of K_m . Compared to Ala-Ala, five of eight substrates (Val-Ala, Leu-Ala, Met-Ala, His-Ala and Arg-Ala) had significantly

reduced k_{cat} values ($p \leq 0.02$). Val-Ala was an extreme example with a k_{cat} of $0.8 s^{-1}$, 43-fold lower than that of Ala-Ala. These reductions in k_{cat} suggest that the transition state is destabilized relative to the ground state for these substrates, possibly as a result of sidechain–subsite interactions altering the position of the scissile amide bond in relation to the Zn(II) ion and catalytically important sidechains.

When catalytic efficiencies (k_{cat}/K_m) are compared (Fig. 1), the specificity conferred by the S1 pocket of PfA-M1 becomes apparent: X-Ala substrates with straight-chain P1 sidechains (Arg, Lys and Met) were most efficiently hydrolyzed, followed by those with larger hydrophobic residues (Phe and Leu). Substrates with P1-Val, -His and -Gly residues were inefficiently hydrolyzed (Fig. 1 and Supplemental Table S1). Pro-Ala exhibited the lowest k_{cat}/K_m measured in this study at $\sim 3 M^{-1} cm^{-1}$, a value that is four orders of magnitude lower than that for the best X-Ala substrates. No hydrolysis of Asp-Ala was detected at high concentrations of enzyme and substrate (Supplemental Table S1). We also tested the substrate Asp-Lys, which has a favorable P1' residue (see next paragraph); no hydrolysis was observed for this substrate either. We then asked whether Asp-Ala binds to PfA-M1 in an orientation that is unproductive for catalysis by assessing whether it acts as a competitive inhibitor; however, we could not detect any inhibition of Leu-Ala hydrolysis in the presence of Asp-Ala at concentrations up to 10 mM.

Variation of the P1' residue in the Ala-X substrate set also had a large effect on K_m whereas the influence on k_{cat} was more muted (Fig. 1). Increasing hydrophobicity of non-polar P1' sidechains correlated with lower K_m ($R^2 = 0.77$; Fig. 2). The presence of the polar sidechains of Thr and Gln in the P1' position resulted in K_m values that were much higher than those observed with non-polar residues. Placement of a charged residue in the P1' position (Ala-Glu) drove the K_m over 100 mM and the k_{cat}/K_m below $100 M^{-1} s^{-1}$ (Supplemental Table S1). Together, these results are consistent with a hydrophobic P1' subsite that is not able to satisfy the hydrogen bonding requirements of small- to medium-sized polar/charged sidechains. However, more distantly located polar groups can clearly be accommodated in the S1' site: K_m values for P1'-Lys and -Met were similar, and a P1'-Tyr residue yielded the lowest K_m of all Ala-X substrates tested. These results suggest that the hydrophobic portion of the Lys and Tyr sidechains are accommodated within the S1' subsite while the ϵ -amino and phenolic hydroxyl groups interact either with solvent or with polar residues in the enzyme. Values for k_{cat} fell within a relatively narrow range ($15\text{--}42 s^{-1}$) with the exceptions of Ala-Thr ($94 s^{-1}$) and Ala-Gln ($5 s^{-1}$). Comparison of catalytic efficiencies (Fig. 1) reveals an S1' subsite that favors sidechains with substantial hydrophobic character. Substrates with P1' residues having polar groups on the β - or γ -carbon of the sidechain (Thr, Gln, Glu) were among the least efficiently cleaved; however, more distantly located polar groups enhanced catalytic efficiency (compare Tyr to Phe). No hydrolysis of Ala-Pro was detected at high concentrations of substrate and enzyme (Supplemental Table S1).

To evaluate the complementarity between various P1 and P1' sidechain groups and the S1 and S1' subsites, respectively, incremental binding free energies were calculated from the k_{cat}/K_m values of selected pairs of substrates (Table 1). The incremental binding free energy is the change in free energy in transferring the group in question from aqueous solvent to a protein environment [19]. These values can then be compared to intrinsic binding energies, which are the maximal binding energies for a given group and reflect a high degree of complementarity between the group and its local environment in a protein binding site. As expected from the hydrophobic nature of the S1 and S1' subsites, transfer of non-polar groups (methyl, isopropyl) from water to the enzyme subsite was thermodynamically favored. However, only a small fraction of the

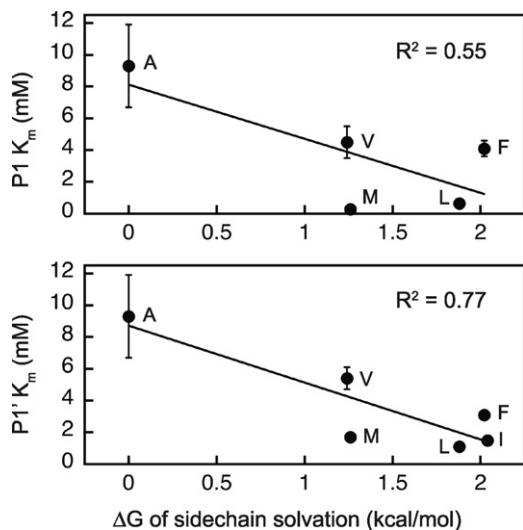


Fig. 2. Relationship between K_m values of X-Ala (upper) and Ala-X (lower) substrate sets and sidechain solvation free energies. Error bars indicate the standard deviations of K_m . The line is a linear regression fit to the data points with the R^2 value indicated.

Table 3
Comparison of kinetic parameters for the hydrolysis of selected X-Ala substrates at pH 5.5 and 7.5.

Substrate	pH	K_m (mM)	k_{cat} (s^{-1})	k_{cat}/K_m ($M^{-1} s^{-1}$)	Ratio ^a
Leu-Ala	7.5	0.64 ± 0.12	9.3 ± 1.0	$(1.4 \pm 0.3) \times 10^4$	12
	5.5	10 ± 3	12 ± 2	$(1.2 \pm 0.4) \times 10^3$	
Arg-Ala	7.5	0.40 ± 0.06	9.5 ± 1.4	$(2.3 \pm 0.5) \times 10^4$	14
	5.5	9.0 ± 2.1	15 ± 2	$(1.7 \pm 0.5) \times 10^3$	
Lys-Ala	7.5	0.43 ± 0.02	27 ± 8	$(6.5 \pm 1.8) \times 10^4$	22
	5.5	8.9 ± 3.0	27 ± 1	$(3.0 \pm 1.0) \times 10^3$	
His-Ala	7.5	4.2 ± 0.9	2.4 ± 0.2	$(5.6 \pm 1.2) \times 10^2$	21
	5.5	35 ± 3	1.0 ± 0.2	27 ± 7	

^a Ratio is the k_{cat}/K_m value at pH 7.5 divided by that at pH 5.5.

available binding energy (one fifth or less) was exploited upon binding to the PfA-M1 subsite. This indicates that the complementarity of the S1 and S1' subsites for the groups examined is far from perfect and suggests that they are not tightly packed in a hydrophobic environment. Transfer of the polar tyrosine hydroxyl group into the S1 subsite was unfavorable, which implies the absence of enzyme groups that are able to hydrogen bond with it. In the S1' pocket, transfer of a Tyr-OH group from water to PfA-M1 was favored, but again the fraction of available binding energy used was low (Table 1).

PfA-M1 produces amino acids from globin peptides in the *P. falciparum* food vacuole [14,15]. Adaptation of PfA-M1 to a role in hemoglobin catabolism may have elicited a shift in substrate specificity such that subsite preferences positively correlate with the abundance of amino acids in human α - and β -globin. To evaluate this possibility, the catalytic efficiencies for hydrolysis of X-Ala and Ala-X substrates were plotted against the abundance of the corresponding P1 or P1' residue, respectively, in α - and β -globin (Fig. 3). In neither case is there a positive correlation between catalytic efficiency of hydrolysis and abundance of the "X" residue in hemoglobin.

3.3. Effect on kinetic parameters of extension of the backbone with glycyl residues and of C-terminal amidation

We have proposed that PfA-M1 catalyzes the hydrolysis of dipeptides generated by a vacuolar dipeptidyl aminopeptidase as well as oligopeptides produced through the concerted action of multiple endopeptidases [6]. To better understand the relationship between substrate length (i.e., number of residues) and catalytic efficiency, the steady-state parameters for hydrolysis of a series of substrates with Leu in the P1 position were determined. The peptide backbone of the reference substrate, Leu-NH₂, was extended with one and two glycyl residues to examine the effects of lengthening the backbone without occupying the S1' or S2' sites. Amidation was employed to swap an H-bond accepting carboxylate oxygen with an H-bond donating amide group. It also eliminated the negative charge at the C-terminus.

Leu-NH₂ was hydrolyzed with moderate catalytic efficiency (Table 2). Extension of Leu-NH₂ by two carbon atoms to Leu-Gly resulted in a 5-fold decrease in K_m and a 3-fold increase in catalytic efficiency. Amidation of the C-terminus of Leu-Gly resulted in a further 7-fold increase in catalytic efficiency (Table 2). Further extension of the backbone to Leu-Gly-Gly had little effect on the kinetic parameters (Table 2). Overall, interactions between PfA-M1 and the substrate P1' and P2' backbone atoms resulted in an order-of-magnitude increase in the catalytic efficiency.

3.4. Substrate interactions with the S2' subsite

To explore the effects of modifying the P2' residue on catalysis, the hydrolysis of Leu-Gly-Gly was compared to that of Leu-Gly-Pro

and Leu-Gly-Leu. The products of hydrolysis (Gly-Gly, Gly-Pro and Gly-Leu) are themselves potentially substrates for further cleavage. However, Gly in the P1 position does not promote efficient catalysis (see Section 3.2) and these dipeptides are likely to be poor substrates for the enzyme. This turned out to be the case, as no free glycine was observed in assays of the three tripeptide substrates.

Both P2' substitutions increased the catalytic efficiency of substrate hydrolysis (Table 2). The changes upon P2' Leu substitution were particularly dramatic, resulting in a 47-fold decrease in K_m and an order of magnitude increase in catalytic efficiency. These results reveal that interaction of the P2' sidechain with a

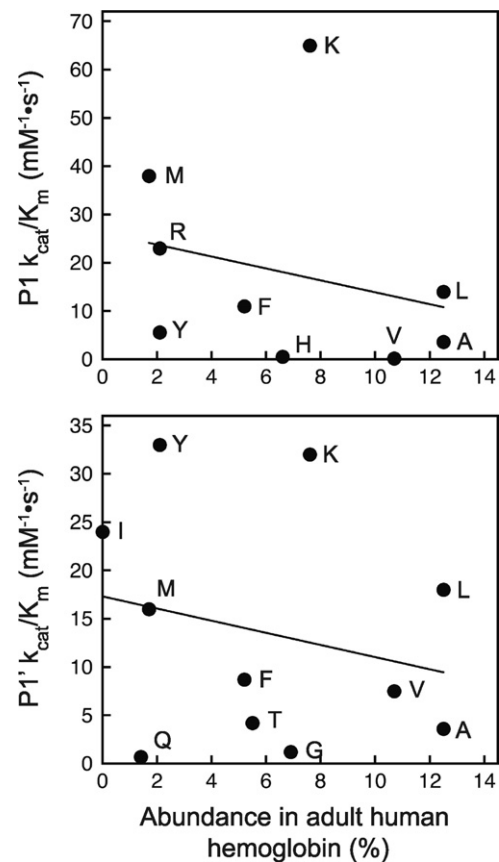


Fig. 3. Relationship between catalytic efficiencies of hydrolysis of X-Ala and Ala-X substrate sets and amino acid abundance in human hemoglobin. For each "X" residue analyzed in the P1 (X-Ala; upper panel) or P1' (Ala-X; lower panel) substrate position, the catalytic efficiency of PfA-M1-catalyzed substrate hydrolysis was plotted against the relative abundance of the amino acid in human hemoglobin (calculated as the percent of the combined amino acid compositions of α - and β -globin). The line is a linear regression fit to the data. The identities of the amino acids are indicated to the right of each data point. Error bars were omitted for clarity.

presumably hydrophobic S2' subsite can contribute substantially to catalytic efficiency.

3.5. Effect of pH on the steady-state parameters of selected X-Ala dipeptides

The lumen of the food vacuole is moderately acidic with a pH of around 5.5 [22–25]. We have previously shown that a change in pH from 7.5 to 5.5 causes the catalytic efficiency of PfA-M1 substrate hydrolysis to decline between 2- and 5-fold for dipeptide substrates and over an order of magnitude for fluorogenic aminoacyl- β -naphthylamide substrates [14]. The primary driver of the reduction in catalytic efficiency was an increase in the K_m values. In this study we have carried out assays at pH 7.5 so that steady-state parameters for substrates with K_m values in the millimolar range could be accurately determined. However, we wanted to assess the kinetic parameters for hydrolysis of selected X-Ala substrates at pH 5.5, particularly those with positively charged (Arg, Lys) or ionizable (His) sidechains, to determine whether a decrease in pH could modulate the S1 subsite specificity.

Kinetic parameters for four X-Ala substrates at pH 7.5 and 5.5 are shown in Table 3. Consistent with our previous studies [14], K_m values increased about an order of magnitude (range: 8- to 23-fold) while changes in k_{cat} were much more modest (≤ 2.4 -fold). These pH-dependent changes in catalytic parameters resulted in decreases in catalytic efficiency of between 12- and 22-fold at pH 5.5 vs. pH 7.5 (Table 3); however, the rank order of catalytic efficiencies remained the same (P1-Lys > Arg > Leu > His) at both pH values. Thus, while pH clearly affected the magnitude of the catalytic efficiencies with which X-Ala peptides were hydrolyzed, the relative values and therefore the S1 subsite specificity remained similar for the substrates examined.

4. Discussion

In this study we have employed an established method for the chromatographic separation and quantitation of amino acids following derivitization with 6-aminoquinolyl-N-hydroxysuccinimidyl carbamate [26] in conjunction with ultra-high pressure liquid chromatography. The speed and high sensitivity offered by this method enabled the determination of steady-state parameters for a large number of substrates with a range in k_{cat}/K_m of ~ 5 orders of magnitude.

Characterization of unmodified peptides offered several advantages over the commonly used fluorogenic aminoacyl conjugates (typically β -naphthylamides or 7-amido-4-methylcoumarins). First, only the S1 subsite can be probed with the fluorogenic substrates because the fluorophore replaces the P1' residue. Second, the range of substrate concentrations that can be assayed is limited by the inner filter effect at high concentrations. Third, we have frequently encountered substrate inhibition when characterizing the kinetics of hydrolysis of fluorogenic amino acyl substrates ([14] and unpublished data). No substrate inhibition was observed with any of the peptide substrates used in this study, which greatly simplified the determination of k_{cat} and K_m . Fourth, Ala is one of the most abundant amino acids in α - and β -globin and X-Ala and Ala-X sequences are likely to be encountered by PfA-M1 in the vacuole, either as dipeptides or as the N-terminal residues of oligopeptides. Finally, it has been observed that subsite specificities determined with non-natural substrates can differ from those observed with peptides [27,28], presumably because the chromophore or fluorophore influences the binding and/or orientation of the substrate in the active site. This seems to be the case for PfA-M1: the S1 specificity determined with aminoacyl-7-amido-4-methylcoumarin substrates was found to have a rank order (highest to lowest k_{cat}/K_m) of Leu > Ala > Arg > Phe [20]. Using

X-Ala dipeptides, we found the order of these P1 residues to be Arg > Leu > Phe > Ala.

Our analysis of 12 X-Ala substrates revealed a preference of the PfA-M1 S1 subsite for basic and hydrophobic residues. Sidechain structure clearly plays a role as well, as indicated by the low efficiency of hydrolysis of Val-Ala. The specificity observed with PfA-M1 is broadly similar to that reported for a number of other M1-family aminopeptidases from prokaryotes (*E. coli* and *Lactobacillus lactis* PepN) and eukaryotes (puromycin-sensitive aminopeptidase, aminopeptidase N and leukotriene A₄ hydrolase (LTA4H), a bifunctional aminopeptidase/hydrolase) [27–32]. Crystal structures of *E. coli* PepN in complex with inhibitors and hydrolysis products (i.e., amino acids) and of an inactive variant of LTA4H bound to a tripeptide substrate have provided insights into the nature of the S1 subsite and its interaction with amino acid sidechains [33–37]. The S1 subsite has been described as a cylinder, with the base corresponding to the site of the enzyme-bound Zn(II) ion [34]. The central region is lined with hydrophobic residues while the “cap” at the end opposite the Zn(II) ion is comprised of two polar sidechains. Non-polar substrate sidechains interact with central hydrophobic region of the cylinder while basic sidechains thread through the hydrophobic cylinder and hydrogen bond with the polar cap residues and nearby water molecules [34,37].

The structure of the S1 subsite of PfA-M1 is very similar to that of *E. coli* PepN [20] and it likely interacts with non-polar and basic substrate P1 sidechains in an analogous manner. The cap residues in PfA-M1 are Glu572 and Met1034 [20]. We speculate that interaction of the positively charged groups of the P1-Arg and -Lys sidechains with Glu572 through hydrogen bonding or salt bridge formation stabilizes these sidechains in the S1 subsite. Any such interactions appear not to be sensitive to pH changes in the range 5.5–7.5, as a preference for basic sidechains in the S1 pocket was observed at both pH values. The structure of the S1 subsite suggests an explanation for why His-Ala was hydrolyzed with a catalytic efficiency two orders of magnitude lower than that of Lys-Ala: the polar His sidechain may not belong enough to interact with the S1 cap but rather may be confined to the hydrophobic central region. A similar argument could be made for the lack of hydrolysis of substrates with P1-Asp.

The preference of PfA-M1 for basic and hydrophobic residues in the P1' position of the substrate is a common feature of M1-family aminopeptidases [27,28,31,32]. The S1' subsite in PfA-M1 and *E. coli* PepN is an open cleft lined with hydrophobic residues [20,33,35] which could stabilize substrate binding by forming van der Waals interactions with non-polar P1' sidechains. Ala-X substrates with small- to medium-size polar and charged P1' residues were hydrolyzed by PfA-M1 with relatively low catalytic efficiency, an effect that was primarily driven by an increase in K_m . This may be due to an incompatibility of these polar residues with the hydrophobic S1' subsite. In contrast, the S1' subsite was able to accommodate the larger polar P1' sidechains Lys and Tyr without an increase in K_m , likely due to the availability of distal hydrogen bonding groups in the enzyme or from solvent. Hydrolysis of Ala-Pro was not detected in our assay, which implies that X-Pro peptides are not physiological substrates of PfA-M1. Rather, amino acid release from substrates with a P1'-Pro residue is catalyzed by the *P. falciparum* homolog of aminopeptidase P, which like PfA-M1 is located in the food vacuole lumen [11].

An analysis of the incremental binding energy of various groups in the S1 and S1' subsites revealed that a relatively low proportion of the available binding energy was utilized. This result indicates that the subsite-substrate interactions, whether hydrophobic interactions with methyl and isopropyl groups or hydrogen bonding interactions with the Tyr-OH group, are not optimized. This is not surprising as the selective pressures on PfA-M1 have likely favored broad tolerance for sidechain size and shape and a subsite that is

highly complementary to a given sidechain would likely exclude many others. One caveat to this analysis is that binding energies for larger groups such as the phenyl group of Phe were not determined due to the lack of availability of the intrinsic binding energy. It is possible that larger sidechains exhibit higher complementarity to the S1 and S1' subsites than those examined in Table 1.

The S2' subsite has not been defined in PfA-M1 but in a co-crystal structure of *E. coli* PepN with a phosphinic tripeptide analog it was identified as a shallow site lined with non-polar residues [35]. Our data suggest that the S2' site of PfA-M1 is non-polar as well, although the sample set was small and no polar or charged residues were tested. Notably, while Pro was strongly disfavored in the P1 and P1' positions, it was well tolerated at P2'.

Interactions with backbone atoms of the substrate also clearly contribute to efficient catalysis. A 20-fold increase in k_{cat}/K_m was observed upon extending Leu-NH₂ to Leu-Gly-NH, which was primarily due to a decrease in K_m . These results imply the presence of stabilizing interactions between PfA-M1 and the amide bond joining the second and third residues of the substrate. In the structure of an inactive mutant of LTA4 with a tripeptide in the active site [37], hydrogen bonds are observed between the P1' carbonyl and two backbone amide hydrogens from residues in the conserved GXMEN motif. In addition, a hydrogen bond is formed between the P2' amide hydrogen and the hydroxyl group of Tyr378, which is conserved as Tyr575 in PfA-M1. We propose that formation of this suite of hydrogen bonds is conserved in the PfA-M1–substrate complex and explains the gains in catalytic efficiency that we observe.

Our data provide a foundation for understanding the role of PfA-M1 in hemoglobin catabolism. The catalytic efficiency of peptide bond hydrolysis increases up to ~200-fold upon occupancy of either the S1 or S1' subsites and up to 10-fold when the S2' subsite is engaged (calculated as the ratio of the highest k_{cat}/K_m at each subsite to that for Gly). Engagement of all three subsites is therefore predicted to lead to high catalytic efficiencies for amide bond hydrolysis. Stated another way, the neighboring sidechains of a given substrate residue should have a large influence on the rate of hydrolysis. There is some evidence that this is the case. We have previously shown dipeptides with hydrophobic amino acids in both of the P1 and P1' positions are hydrolyzed with high catalytic efficiency ($k_{cat}/K_m \sim 10^5 \text{ M}^{-1} \text{ s}^{-1}$) [14], as would be predicted from the S1 and S1' specificities defined here. The importance of context is further exemplified by comparing two substrates with a P1'-Gly residue from this study. Ala-Gly was a relatively poor substrate with a k_{cat}/K_m of $120 \text{ M}^{-1} \text{ cm}^{-1}$. When a P1'-Gly was flanked by two Leu residues (Leu-Gly-Leu), the substrate was hydrolyzed three orders of magnitude more efficiently. Thus, the accretion of binding energy across multiple enzyme subsites likely contributes to the efficient hydrolysis of a large proportion of the di- and oligopeptides generated from α - and β -globin in the food vacuole. It also explains why the S1 and S1' subsite specificities do not need to correlate with the abundances of amino acids in hemoglobin: when it comes to complex mixtures of physiological substrates, subsite specificities defined with model substrates likely overestimate the significance of the preferences of any individual subsite.

Acknowledgments

We are grateful to M. Hernick for access to the ion chromatography system and to members of the Klemba lab for critical reading of the manuscript. This work was supported by grant R01AI077638 from National Institutes of Allergy and Infectious Diseases (M.K.).

Appendix A. Supplementary data

Supplementary data associated with this article can be found, in the online version, at doi:10.1016/j.molbiopara.2012.02.003.

References

- [1] Fournie-Zaluski MC, Fassot C, Valentin B, Djordjijevic D, Reaux-Le Goazigo A, Corvol P, et al. Brain renin-angiotensin system blockade by systemically active aminopeptidase A inhibitors: a potential treatment of salt-dependent hypertension. *Proc Natl Acad Sci USA* 2004;101:7775–80.
- [2] Penning TD. Inhibitors of leukotriene A4 (LTA4) hydrolase as potential anti-inflammatory agents. *Curr Pharm Des* 2001;7:163–79.
- [3] Bauvois B, Dauzonne F D. Aminopeptidase-N/CD13 (EC 3.4.11.2) inhibitors: chemistry, biological evaluations, and therapeutic prospects. *Med Res Rev* 2006;26:88–130.
- [4] Snow RW, Craig M, Deichmann U, Marsh K. Estimating mortality, morbidity and disability due to malaria among Africa's non-pregnant population. *Bull World Health Organ* 1999;77:624–40.
- [5] Hanssen E, Knoechel C, Dearnley M, Dixon MW, Le Gros M, Larabell C, et al. Soft X-ray microscopy analysis of cell volume and hemoglobin content in erythrocytes infected with asexual and sexual stages of *Plasmodium falciparum*. *J Struct Biol* 2011, doi:10.1016/j.jsb.2011.09.003.
- [6] Dalal S, Klemba M. Roles for two aminopeptidases in vacuolar hemoglobin catabolism in *Plasmodium falciparum*. *J Biol Chem* 2007;282:35978–87.
- [7] Goldberg DE. Hemoglobin degradation. *Curr Top Microbiol Immunol* 2005;295:275–91.
- [8] Klemba M, Gluzman I, Goldberg DE. A *Plasmodium falciparum* dipeptidyl aminopeptidase I participates in vacuolar hemoglobin degradation. *J Biol Chem* 2004;279:43000–7.
- [9] Rosenthal PJ. Cysteine proteases of malaria parasites. *Int J Parasitol* 2004;34:1489–99.
- [10] Schechter I, Berger A. On the size of the active site in proteases. I. Papain. *Biochem Biophys Res Commun* 1967;27:157–62.
- [11] Ragheb D, Bompiani K, Dalal S, Klemba M. Evidence for catalytic roles for *Plasmodium falciparum* aminopeptidase P in the food vacuole and cytosol. *J Biol Chem* 2009;284:24806–15.
- [12] Florent I, Derhy Z, Allary M, Monsigny M, Mayer R, Schrevel J. A *Plasmodium falciparum* aminopeptidase gene belonging to the M1 family of zinc-metalloproteases is expressed in erythrocytic stages. *Mol Biochem Parasitol* 1998;97:149–60.
- [13] Azimzadeh O, Sow C, Geze M, Nyalwidhe J, Florent I. *Plasmodium falciparum* PfA-M1 aminopeptidase is trafficked via the parasitophorous vacuole and marginally delivered to the food vacuole. *Malar J* 2010;9:189–205.
- [14] Ragheb D, Dalal S, Bompiani KM, Ray WK, Klemba M. Distribution and biochemical properties of an M1-family aminopeptidase in *Plasmodium falciparum* indicate a role in vacuolar hemoglobin catabolism. *J Biol Chem* 2011;286:27255–65.
- [15] Harbut MB, Velmourougane G, Dalal S, Reiss G, Whisstock JC, Onder O, et al. Bestatin-based chemical biology strategy reveals distinct roles for malaria M1- and M17-family aminopeptidases. *Proc Natl Acad Sci USA* 2011;108:E526–34.
- [16] Flipo M, Beghyn T, Leroux V, Florent I, Deprez BP, Deprez-Poulain RF. Novel selective inhibitors of the zinc plasmoidal aminopeptidase PfA-M1 as potential antimalarial agents. *J Med Chem* 2007;50:1322–34.
- [17] Flipo M, Florent I, Grellier P, Sergheraert C, Deprez-Poulain R. Design, synthesis and antimalarial activity of novel, quinoline-based, zinc metallo-aminopeptidase inhibitors. *Bioorg Med Chem Lett* 2003;13:2659–62.
- [18] Atanassova A, Lam R, Zamble DB. A high-performance liquid chromatography method for determining transition metal content in proteins. *Anal Biochem* 2004;335:103–11.
- [19] Fersht A. Enzyme structure and mechanism. 2nd ed. New York: W.H. Freeman; 1985.
- [20] McGowan S, Porter CJ, Lowther J, Stack CM, Golding SJ, Skinner-Adams TS, et al. Structural basis for the inhibition of the essential *Plasmodium falciparum* M1 neutral aminopeptidase. *Proc Natl Acad Sci USA* 2009;106:2537–42.
- [21] Fauchère J-L, Pliška V. Hydrophobic parameters of pi amino-acid side chains from the partitioning of N-acetyl-amino acid amides. *Eur J Med Chem Chim Ther* 1983;18:369–75.
- [22] Bennett TN, Kosar AD, Ursos LM, Dzekunov S, Singh Sidhu AB, Fidock DA, et al. Drug resistance-associated pfcRT mutations confer decreased *Plasmodium falciparum* digestive vacuolar pH. *Mol Biochem Parasitol* 2004;133:99–114.
- [23] Klonis N, Tan O, Jackson K, Goldberg D, Klemba M, Tilley L. Evaluation of pH during cytosomal endocytosis and vacuolar catabolism of hemoglobin in *Plasmodium falciparum*. *Biochem J* 2007;407:343–54.
- [24] Krogstad DJ, Schlesinger PH, Gluzman IY. Antimalarials increase vesicle pH in *Plasmodium falciparum*. *J Cell Biol* 1985;101:2302–9.
- [25] Kuhn Y, Rohrbach P, Lanzer M. Quantitative pH measurements in *Plasmodium falciparum*-infected erythrocytes using pHluorin. *Cell Microbiol* 2007;9:1004–13.
- [26] Cohen SA, Michaud DP. Synthesis of a fluorescent derivatizing reagent, 6-aminoquinolyl-N-hydroxysuccinimidyl carbamate, and its application for the analysis of hydrolyzable amino acids via high-performance liquid chromatography. *Anal Biochem* 1993;211:279–87.
- [27] Niven GW, Holder SA, Stroman P. A study of the substrate specificity of aminopeptidase N from *Lactococcus lactis* subsp. cremoris Wg2. *Appl Microbiol Biotechnol* 1995;44:100–5.
- [28] Orning L, Gierse JK, Fitzpatrick FA. The bifunctional enzyme leukotriene-A4 hydrolase is an arginine aminopeptidase of high efficiency and specificity. *J Biol Chem* 1994;269:11269–73.

- [29] Drag M, Bogyo M, Ellman JA, Salvesen GS. Aminopeptidase fingerprints, an integrated approach for identification of good substrates and optimal inhibitors. *J Biol Chem* 2010;285:3310–8.
- [30] Huang K, Takahara S, Kinouchi T, Takeyama M, Ishida T, Ueyama H, et al. Alanyl aminopeptidase from human seminal plasma: purification, characterization, and immunohistochemical localization in the male genital tract. *J Biochem* 1997;122:779–87.
- [31] Johnson GD, Hersh LB. Studies on the subsite specificity of the rat brain puromycin-sensitive aminopeptidase. *Arch Biochem Biophys* 1990;276:305–9.
- [32] Chappelet-Tordo D, Lazdunski C, Murgier M, Lazdunski A. Aminopeptidase N from *Escherichia coli*: ionizable active-center groups and substrate specificity. *Eur J Biochem* 1977;81:293–305.
- [33] Addlagatta A, Gay L, Matthews BW. Structure of aminopeptidase N from *Escherichia coli* suggests a compartmentalized, gated active site. *Proc Natl Acad Sci USA* 2006;103:13339–44.
- [34] Addlagatta A, Gay L, Matthews BW. Structural basis for the unusual specificity of *Escherichia coli* aminopeptidase N. *Biochemistry* 2008;47:5303–11.
- [35] Fournie-Zaluski MC, Poras H, Roques BP, Nakajima Y, Ito K, Yoshimoto T. Structure of aminopeptidase N from *Escherichia coli* complexed with the transition-state analogue aminophosphinic inhibitor PL250. *Acta Crystallogr D* 2009;65:814–22.
- [36] Ito K, Nakajima Y, Onohara Y, Takeo M, Nakashima K, Matsubara F, et al. Crystal structure of aminopeptidase N (proteobacteria alanyl aminopeptidase) from *Escherichia coli* and conformational change of methionine 260 involved in substrate recognition. *J Biol Chem* 2006;281:33664–76.
- [37] Tholander F, Muroya A, Roques BP, Fournie-Zaluski MC, Thunnissen MM, Haegstrom JZ. Structure-based dissection of the active site chemistry of leukotriene A4 hydrolase: implications for M1 aminopeptidases and inhibitor design. *Chem Biol* 2008;15:920–9.